Effect of Surface Biopolymeric Treatment on Sisal Fiber Properties and Fiber-Cement Bond

Paulo R. L. Lima, PhD, Heni Mirna Santos, Geany Peruch Camilloto, PhD, Renato Souza Cruz, PhD

State University of Feira de Santana Technology, Feira de Santana, Bahia BRAZIL

Correspondence to:
Paulo R.L. Lima email: lima.prl@pq.cnpq.br

ABSTRACT

Sisal fiber, available in various semi-arid regions around the world, is the most studied natural fiber for the reinforcement of polymeric and cement-based composites. However, to improve the fiber–matrix interaction and to reduce the hydrophilicity of the fiber, it is necessary to establish surface treatments that employ sustainable materials, unlike conventional surface treatments. In this work, sisal fibers were coated separately with cellulose acetate, hydrophobic starch, and cassava starch biopolymers in order to verify the possibility of reducing the water absorption capacity of the fiber by the use of a biodegradable resin. A combination of Fourier transform infrared spectroscopy, scanning electron microscopy, and water absorption and tensile tests was used to investigate the effects of the surface treatments on the sisal fiber properties. Pullout tests of sisal fibers with embedded lengths of 20 mm and 40 mm were performed to determine the influence of the treatments on the bond stress with cement mortar. Composites with 4 vol % short fiber were produced and tested for flexion. The study results indicated that all treatments reduced the mechanical properties of the fiber; however, the layer of the cellulose acetate biopolymer film formed on the fiber surface was effective in reducing the fiber hydrophilicity. Experimental tests on the composites revealed that the cellulose acetate treatment reduced the bond stress and, to a lesser degree, the flexural toughness of the composite, despite the increase in flexural strength.

Keywords: natural fiber, fiber treatment, composites, pullout test

INTRODUCTION

In the last few decades, natural fiber has increasingly been used as a reinforcement of composites owing to its ability to lend stiffness, strength, and toughness to the composites [1, 2, 3, 4, 5]. Given the excellent mechanical properties of sisal fiber—which is extracted from the *Agave sisalana* leaf—it is one of the most important fibers used as reinforcement [6]. Classification of patent documents involving sisal fibers, which were extracted from the Derwent Innovation Index database, between 1960 and 2009 revealed the existence of 1373 records, about 7.4% of which were associated with the use of this fiber as a reinforcement of composites [7]. Sisal fiber has an advantage over other natural fibers in that it is commercially produced in many countries, which facilitates its immediate use for the large-scale production of building elements. Because of the versatility of sisal fiber, it has been employed in pulp, short fiber, long fiber, and fabric forms in cement-based composites [8-11].

However, the most serious concern about natural fibers is their hydrophilic nature, which is attributed to the presence of pendant hydroxyl and polar groups in various constituents of these fibers; this property can lead to poor adhesion between the fibers and a matrix [12, 13]. Sisal fibers have high water absorption capacity [14]; thus, their swelling and shrinking due to wetting and drying of the composites in use may lead to cracking at the fiber–matrix interface. As loads are applied directly to the matrix, it is necessary to ensure an effective load transfer from the matrix to the fibers in order to ensure good mechanical behavior of the composites. As a result, the mechanical properties of natural-fiber-reinforced composites are highly sensitive to moisture content and an increase in this property is associated with reductions in the elastic modulus and strength of the composite [15-17]. In addition, dimensional changes of cement composites due to loss of water are altered by the presence of hygroscopic natural fibers; this intensifies the extent of shrinkage strain, in relation of dimensional changes of the cement matrix [18].

Two main types of fiber treatment are commonly employed for reducing the hydrophilicity of the fiber: bulk and surface treatments. The fundamental difference between these treatments is to be found not in the underlying chemistry but in the fact that the

former treatment leads to a radical transformation of the entire fiber, which almost always modifies its morphology and semicrystalline phase, whereas the latter keeps these features virtually intact, except for the formation of an extremely thin outer layer [19].

Bulk treatments of natural fibers, e.g., heat treatment of sisal fibers by the application of wetting-drying cycles [20] or mechanical pressure [21], result in modification of the cellulose structure and reduction in the fiber area and lumen dimensions and consequently reduce moisture absorption.

Surface treatment of natural fibers with various coupling agents is the more commonly used method for improving the fiber–matrix interaction. Coupling agents are molecules that possess two functions: the first is to react with OH groups of cellulose (pore sealing) and the second is to react with functional groups of which causes an increase in the number of chemical links [22]. Coupling agents usually improve the degree of crosslinking in the interface region and provide perfect bonding [23]. Several studies have reported on the effects of surface treatment of sisal fibers with various coupling agents on enhancement of the fiber durability and fiber–matrix interaction. For example, Canovas et al. [24] used timber extracts (colophony, tannin, and vegetable oil) to impregnate sisal fiber; this approach provided good results in terms of a reduction of more than 50% in the water absorption capacity of the fiber despite a small reduction in its tensile strength. Flexural test results showed that mortar reinforced with impregnated fibers exhibited better durability behavior than that reinforced with unimpregnated fibers. Toledo Filho et al. [25] evaluated the effects of treatment of aligned long sisal fiber with slurried silica fume on the durability of cement-based composites and verified that this treatment is an effective method for improving the strength and toughness of the composites with time. Silane coupling agents have been found to be effective in modifying the natural fiber–matrix interface; silane treatment of sisal fibers changes their surface topography, surface chemical structure, and thermal degradation [26; 27]. Singh et al. [28] used gamma-methacryloxypropyl trimethoxy silane as a coupling agent and verified that the moisture absorption of the surface-treated fibers reduced significantly on account of the hydrophobicity provided to the surface by long-chain hydrocarbon attachment.

Despite the relative success of surface treatments in reducing the water absorption capacity of fibers and improving the fiber–matrix interface, there is an apparent contradiction in the use of synthetic polymers with natural fibers. In this scenario, the key environmental advantages of fibers, such as their biodegradability and renewability, reduce or cease altogether. The exhaustive use of petroleum-based resources has led to efforts being initiated toward the development of biopolymers that are generated from renewable natural sources, which are often biodegradable and nontoxic [29, 30]. On account of the beneficial environmental and technical properties of these biopolymers, they have been used in combination with biofibers such as kenaf, hemp, flax, jute, henequen, and sisal to produce polymeric composites [31-34].

Treatment of natural fiber with biotechnological products (enzyme) yields long, thick hydrophobic fibers with extremely low water absorption capacity [35]. This demonstrates that it is possible to use biotreatments to improve the properties of fibers for use in composites.

The aim of the present study was to evaluate the effects of treatment of sisal fiber with biopolymers on the properties of the fiber and cement-based composites. Fiber modification was evaluated via Fourier transform infrared (FTIR) spectroscopy, scanning electron microscopy (SEM), water absorption tests, and tensile tests. Mechanical interactions between a matrix and its fiber reinforcement were discussed on the basis of results of pullout tests. The mechanical performance of cement-based composites reinforced with 4 vol% treated fiber was also studied.

EXPERIMENTAL PROGRAM

Fiber Treatment

The sisal fibers (*Agave sisalana*) used in the present study was collected from Valente city in the state of Bahia, Brazil. Initially, the fibers were washed in hot water (50°C) to remove surface residues, such as mucilages, from the extraction process.

Cellulose and starch are some of the most abundantly available materials on earth that are used as biopolymers on account of their excellent chemical and physical properties. Both starch and cellulose are carbohydrates that are classified as polysaccharides since they are composed of chains of glucose molecules. Cellulose is a molecule found in plants that are made up entirely of repeating glucose units. The main difference between starch and cellulose is in their bond structures, as shown in *Figure 1*.

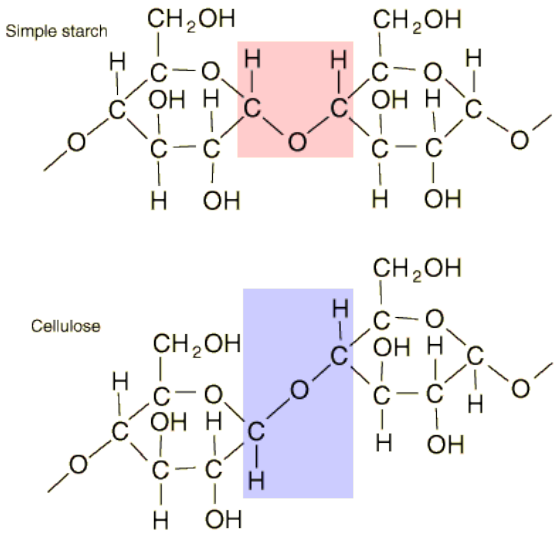

FIGURE 1. Structural formulas of starch and cellulose [36].

In this work, three biopolymers were used to treat sisal fiber (see *Figure 2a*): cellulose acetate (CA), hydrophobic starch (HS), and cassava starch (CS).

For production of CA gel, CA was successfully solubilized in acetone (in the proportion of 1 g in 10 ml) for 24 h. HS gel was prepared by gelatinization in 1% NaOH solution by manual shaking. For production of CS gel, starch dispersions were previously prepared with 8 g of starch per 100 g of water. The starch gelatinization was achieved via thermal treatment at 65 °C for 3 min.

Fiber treatment entailed consisted of their immersion in a biopolymer gel (see *Figure 2b*) and subsequent drying in alignment for 24 h.

FIGURE 2. Treatment of fiber: a) biopolymeric gels; b) immersion of fiber.

Matrix and Composites

CPV-ARI Portland cement (ASTM Type III), silica fume, and fly ash, with specific masses of 3.06 kg/dm^3, 2.11 kg/dm^3, and 2.28 kg/dm^3, respectively, were used for the production of the cement matrix. The use of pozzolans in cement matrices results in the consumption of calcium hydroxide, thereby preventing the occurrence of fiber mineralization [37]. The use of fly ash is also aimed at ensuring greater workability of the matrix, which would facilitate better fiber dispersion [20]. Quartz sand with a specific mass of 2.62 kg/dm^3 was used as fine aggregate in this study. The maximum dimension of sand was 1.18 mm and the thinness modulus was 1.79.

To build the cement matrix, the proportion by weight of 0.5:0.1:0.4:1:0.35 (cement:silica:fly ash:sand:water) was used. A third-generation polycarboxylate superplasticizer, acquired from Vedacit, was used at a dosage of 0.8% (solid of superplasticizer/cementitious materials) to ensure good workability of the mixture. The viscosity modifier Rheomac UW 410 was used at a dosage of 0.6 kg/m^3 in order to avoid segregation during molding. The matrix used in this study showed a flow table spreading of 400 ± 10 mm, as determined according to NBR 13276/05 [38].

The mixture was produced in a mechanical mixer with a volume of 20 dm³ according to the following procedure: 30 s at low speed to add the cementitious products, 30 s at low speed to add the sand, 90 s stopped to scrape the walls of the bowl, and 60 s at high speed.

Cement-based composites reinforced with 4 vol% (by volume) sisal fiber with a length of 40 mm were subjected to flexural testing. For production of the composites, the sisal fibers were manually added to the matrix, mixed for 4 min, and cast into the metallic mold.

Test Methods

The fiber diameter was determined using an optical microscope (QUIMIS, Q711FT). The fiber strands were observed under 10X optical lens; finally, the monostrand was photographed with a camera attached to the microscope. Then, the photograph was transferred to the Motic Images Plus 2.0 imaging software, where the fiber diameter was measured.

FTIR spectroscopy was used to analyze the change in the chemical composition of the treated sisal fiber in comparison to that of natural sisal fiber. FTIR spectra were measured in the wavenumber range of 4000 cm^{-1} to 400 cm^{-1} on a Perkin-Elmer spectrometer.

For the water absorption tests, the specimens were removed from water, wiped dry to remove surface moisture, and then weighed using an electronic balance accurate to 0.1 mg to monitor the mass

during time *t*. The moisture content absorbed by each specimen (*Abs*) was calculated from its weight before (w_0) and after (w_t) absorption as follows:

$$Abs\ (\%) = 100(w_t - w_0)/w_0 \quad (1)$$

Tensile tests of the fiber and film, shown in *Figures 3a and 3b*, respectively, were performed according to a previously reported procedure [20]. The tensile tests were performed using a TA.XT Plus texture analyzer with a load capacity of 500 N and a displacement speed of 0.03 mm/s for the fibers and 0.08 mm/s for the films. For each treatment, 15 fibers with a length of 30 mm each were employed. A total of 10 specimens of each type of biopolymer film were tested.

The CA, CS, and HS films were produced by the casting method. The gels were spread on glass plates and dried at room temperature (25 ± 2 °C). After total evaporation of the solvent, the films were removed and stored. The film used in the tensile test had a length of 50 mm and width of 20 mm. The film thickness was different for different types of resin used: 0.02 mm for the CA film, 0.09 mm for the HS film, and 0.07 mm for the CS film.

The pullout tests were performed using a previously reported methodology [39]. The embedded lengths of the fiber were 20 mm and 40 mm. The specimens were molded using plastic tubes 20 mm in diameter (Figure 3c). After the mold was filled with the matrix, the top cap was fixed and the fiber was stretched slightly for alignment. The mortar was placed in plastic bags before being placed in the mold so as to facilitate the casting process. The pullout test was performed in the TA.XT Plus texture analyzer with a displacement rate of 0.02 mm/s after water curing for 14 days. The bond strength (τ) was calculated using the following equation:

$$\tau = P/(\pi \cdot d \cdot L_f) \quad (2)$$

where *P* is the maximum load, *d* is the average fiber diameter, and L_f is the embedded length of the fiber.

Four-point bending tests, shown in *Figure 3d*, were performed in a Shimadzu testing machine. A load cell of 2 kN was used, and the machine was controlled at a displacement rate of 0.5 mm/min. Three specimens, each with dimensions of 400 mm × 80 mm × 1.2 mm, were tested for each mixture. The load and mid-span displacement, which was measured using a linear variable displacement transducer (LVDT), were continuously recorded using a data acquisition system. The tests were performed after 28 days of water immersion of the specimens. The flexural strength and toughness index *FT* (area under the curve for displacements of 2 mm and 5 mm) were obtained from the stress–displacement curves.

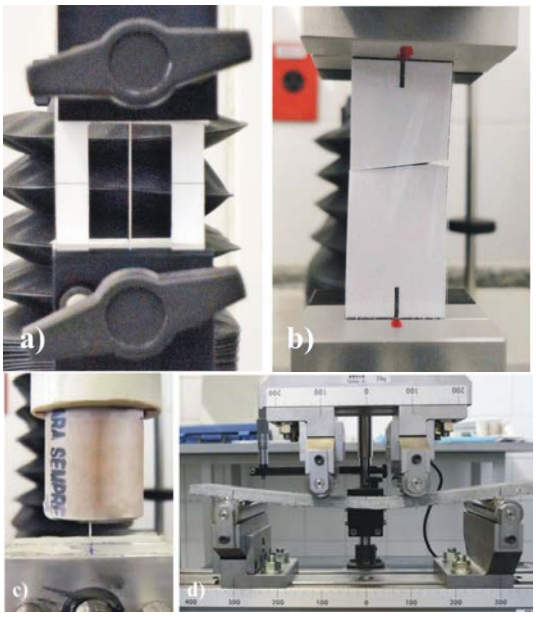

FIGURE 3. Test setup: a) tension of fiber; b) tension of film; c) pull out; d) flexural of composite

RESULTS AND DISCUSSION

Analysis of Fibers and Biopolymer Films

The changes in the surface morphology of the treated fiber were evaluated by SEM observations. In SEM images of natural sisal fiber (*Figures 4a and 4b*), the presence of parenchymatous cells and residual impurities of sisal leaf is observed. After treatment, the formation of a polymer film around the fiber (*Figure 4b*) and the extraction of these surface constituents can be observed. As a direct result, the fiber has a smoother texture and lower surface roughness. An increase in the fiber diameter is also observed (*see Figure 5*), which is attributed to the formation of the polymer film around it.

The change in the chemical composition of the fiber surface can be observed in the FTIR spectra of the untreated and treated sisal fibers shown in *Figure 6*. In the natural fiber, the carbonyl peak at 1735 cm^{-1} is assigned to C=O unconjugated stretching of the carboxylic acid or ester of the hemicelluloses and the peak at 1239 cm^{-1} is assigned to the C–O stretching vibration of the acyl group present in the lignin [41, 42]. The broad peak in the range of 3300–3500 cm^{-1} and a peak at 1630 cm^{-1} are attributed to the characteristic axial vibration of the hydroxyl group of cellulose (preferably from 2, 3 and 6 carbon of

glucose). The peak at around 1080 cm^{-1} is due to the associated hydrogen group [43]. The peak at 1035 cm^{-1} can be attributed to the -C-O-C- stretching [44]. The band at 2922 cm^{-1} is assigned to CH_2 symmetric stretching vibrations.

Evaluation of the FTIR spectra indicates a chemical modification of the sisal fiber surface that was subjected to treatments. The spectra of the treated fibers are found to be different from those of the untreated fiber; these differences vary according to the different types of film used.

In the case of CA treatment, the decreasing intensity of characteristic bands assigned to hydroxyl groups at 3445 cm^{-1} and a reduction of peaks between 1288 cm^{-1} and 1500 cm^{-1} confirm the alteration of the fiber surface. In addition, the peak at 1239 cm^{-1}, which is assigned to the C–O stretching vibration of the acyl group present in the lignin, is shifted after treatment. The FTIR spectrum of the fiber subjected to HS treatment shows the presence of new peaks at 1078 cm^{-1} and 1015 cm^{-1}, which are characteristic of anhydroglucose rings [45]. In the case of CS treatment, a reduction in peaks in the ranges of 3300–3500 cm^{-1} and 1050–2000 cm^{-1}, accompanied by the disappearance of the peak at 897 cm^{-1}, is observed.

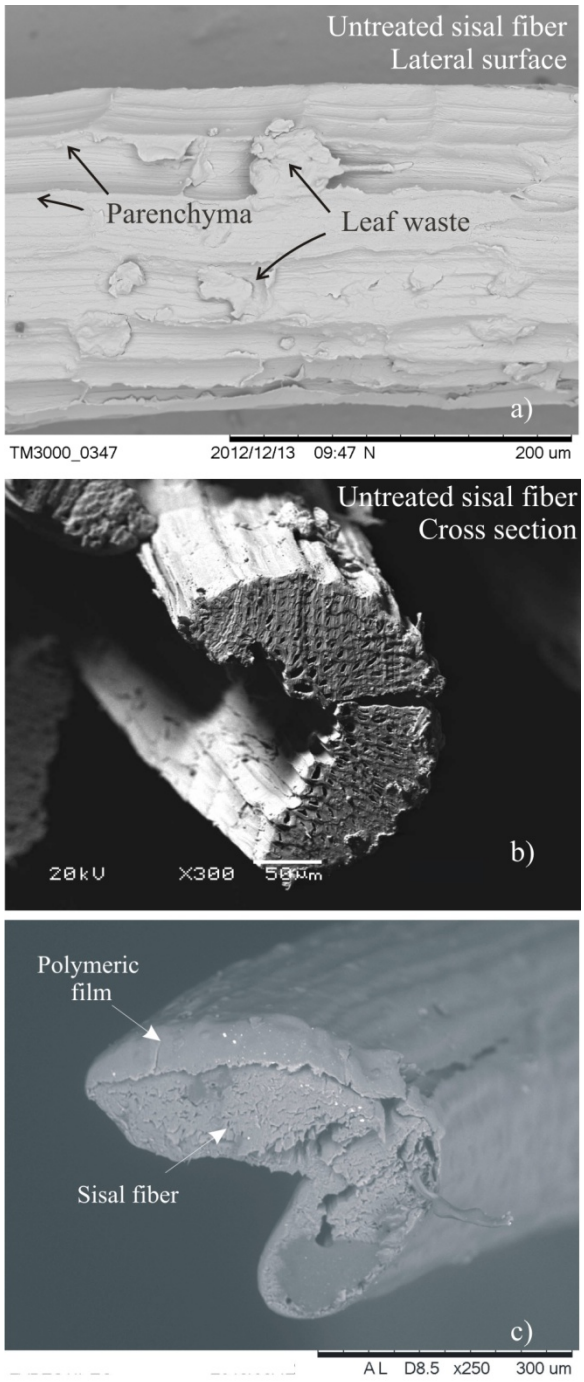

FIGURE 4. Effect of treatment on surface texture of sisal fiber: a,b) untreated fiber; b) treated fiber.

Figure 7a shows the water absorption capacity of the sisal fiber subjected to different treatments at the time of 3 h. The treatments of the fiber with the CS and HS biopolymers cause a considerable increase in the water absorption capacity of the fiber, indicating that these biopolymer films are more hydrophilic than natural sisal fiber. Treatment with the CA biopolymer, however, promotes the formation of a coating layer that significantly reduces the water absorption capacity as a function of time, as shown in *Figure 7b*. After 9 days of immersion, the maximum water absorption capacity of the sisal fiber treated with the CA biopolymer is 88%, whereas that of the natural sisal fiber is about 200%. Ferreira et al. [46] achieved a reduction of 200%–150% in the water absorption capacity of sisal fiber after its impregnation in an aqueous solution with a styrene butadiene polymer. This demonstrates that the CA film obtained from a renewable source is more efficient in reducing sisal fiber absorption than is the polymer film derived from fossil fuel used by Ferreira et al. [46].

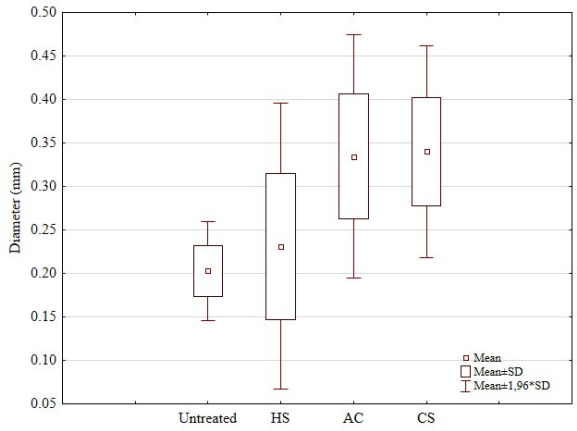

FIGURE 5. Variation of fiber diameter.

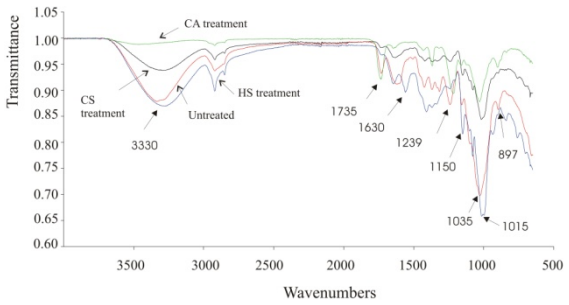

FIGURE 6. Fourier transform infrared (FTIR) spectrum for treated and untreated sisal fiber.

The sisal fibers and polymer films were subjected to tensile tests in order to investigate the influence of the surface treatments on the mechanical behavior of the fibers. Typical stress–strain curves for the biopolymer films and for the fibers subjected to each treatment are shown in *Figure 8* and *Figure 9*, respectively. Results for only a few specimens are shown for ease of viewing. The tensile strength, ultimate strain, and elastic modulus obtained from the experimental curves are presented in *Table I*.

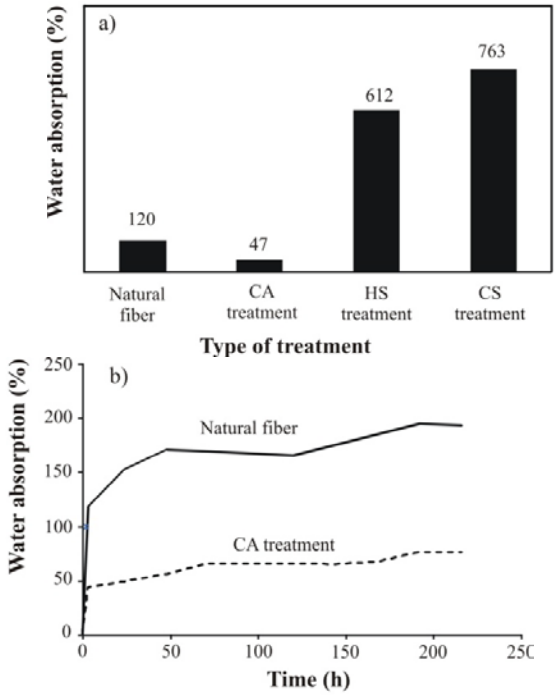

FIGURE 7. Effect of treatment on water absorption of sisal fiber after : a) 3h; b) 9 days.

The CA, HS, and CS films exhibited different mechanical behaviors; this could be easily observed from the results of the tensile tests shown in *Figure 8*. All films exhibited a nonlinear behavior under traction; however, the tensile failure stress–strain curves showed that the CA and HS films exhibited more brittle behavior whereas the CS film showed rupture at a higher deformation. The CA film showed a higher tensile strength and elastic modulus than the other two films, as presented in *Table I*, but its tensile strength was only 15% of that of the sisal fiber. The elastic modulus of the films ranged from 1.84 GPa to 4.50 GPa whereas that of the sisal fiber was 21.44 GPa. The tensile strength of the CS film was similar to that determined in a previous study [47].

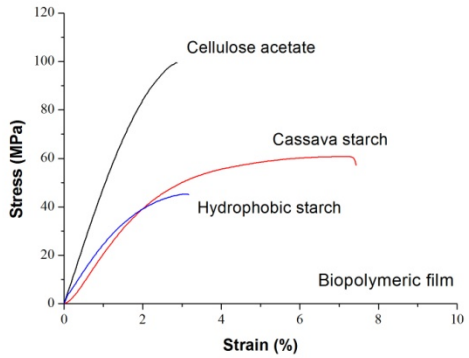

FIGURE 8. Typical stress-strain behavior of biopolymeric films.

In can be seen in *Figure 9* that the untreated and treated fibers exhibited brittle behavior, similar to that reported in the literature [48, 49], with a sudden load drop despite the latter being coated with a polymer film.

Examination of the effects of surface biopolymer treatment on the mechanical properties of sisal fiber as listed in *Table I* indicates reductions in the tensile strength (up to 35%), elastic modulus (up to 39%), and ultimate strain (up to 18%) of the fiber. Treated fiber, shown in *Figure 4*, may be considered as a composite material with a fiber core that is covered with a polymeric material. In this context, its properties are linearly proportional to the properties of each component material and they can be estimated by a micromechanics approach termed the rule of mixtures [50]. In fact, *Figure 10* shows that the tensile strength and elastic modulus of the treated fibers are proportionately reduced in comparison to those of natural sisal fiber.

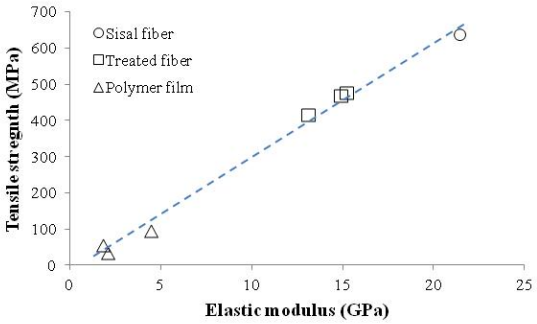

FIGURE 10. Correlation between mechanical properties for untreated fiber, film and treated fiber.

Pullout Test

From the absorption test results, it was observed that the CS and HS biopolymers cannot be used as coupling agents in the treatment of sisal fiber owing to their higher water absorption capacities. Therefore, pullout tests were performed on the untreated fiber and the fiber treated with the CA biopolymer. Typical curves obtained from the pullout tests are shown in *Figure 11*.

On the basis of several sets of experimental results, the pullout behavior can be described by a schematic pullout curve, according to a previous study [46], with four distinct regions (see *Figure 11*). Here, Region 1 corresponds to the elastic bond, with a linear relationship between the load and the slip. The end of this region is characterized by a nonlinear behavior of the curve, which defines the initial point of fiber debonding. With an increase in the load in Region 2, the peak response is attained in Region 3 under partial debonding conditions, where the pullout force reaches a maximum value (*P*). For a given matrix and fiber, the post-peak behavior depends on the embedded length and diameter of the fiber. In this study, a stronger adhesion bond is observed for sisal fibers with a length of 40 mm, which results in fiber fracture, as shown in *Figure 11*. The nominal shear strength computed at *P* by using Eq. (2) is presented in *Table II*.

TABLE I. Experimental tensile results (coefficient of variation, in %, between parentheses).

Material	Treated fiber			Biopolymeric film		
	Tensile strength (MPa)	Ultimate strain (%)	Elastic modulus (GPa)	Tensile strength (MPa)	Ultimate strain (%)	Elastic modulus (GPa)
Natural fiber	639.01 (18.56)	4.07 (26.76)	21.44 (11.14)	-	-	-
Cellulose Acetate	475.42 (21.64)	3.37 (13.39)	15.20 (32.07)	96.04 (24.95)	3.60 (44.20)	4.50 (13.29)
Cassava Starch	415.92 (27.05)	3.97 (29.90)	13.09 (55.30	55.11 (13.09)	6.84 (28.64)	1.84 (29.60)
Hydrophobic starch	467.78 (16.00)	3.60 (16.31)	14.93 (29.27)	34.30 (1.97)	3.17 (9.91)	2.09 (13.33)

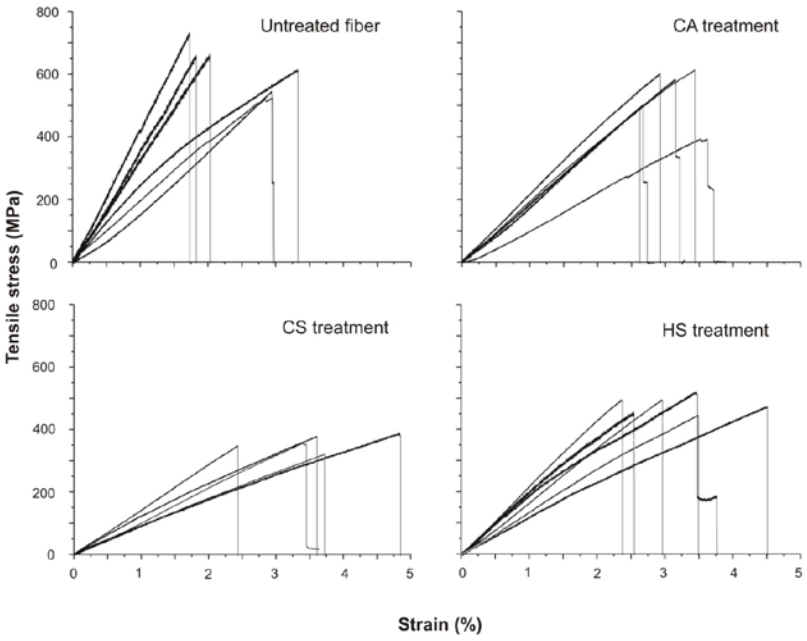

FIGURE 9. Effect of treatment on stress-strain behavior of sisal fiber.

For the 20-mm-long sisal fiber, however, a steep drop in the load–slip curve after attainment of the peak load indicates the end of the debonding of the elastic bond, and the residual pullout force is characteristic of the initial frictional resistance to the pullout of the reinforcement. The pullout behavior in the post-peak region (Region 4) is governed by the frictional shear strength of the interface, and it continues until the fiber is completely debonded from the interface. This zone is characterized by a "stick-slip" behavior, which occurs when the ductile fiber is drawn from the brittle matrix. While 40mm-long natural fiber shows an abrupt drop of load-slip due catastrophic rupture of fiber, the 20mm-long fibers show gradual debonding while the fiber is being extracted from the matrix.

The polymer treatment of the sisal fiber results in changes in the load–slip behavior, as can be seen in Figure 11. A significant reduction in rigidity is observed in Region 1, which is represented by a decrease in the linear slope portion and a reduction in the peak load in comparison to that when the untreated fiber is pulled out. As the treated fibers are coated with a polymer film, their behavior under loading is influenced by three factors: the interface between the CA polymer and the cement matrix, the stiffness of the polymer film under loading, and the fiber–polymer interface.

The chemical structure of CA polymer makes it hydrophobic, leading to weakened bonding with cement matrix. However, in this work, we found that the CA polymer film has lower water absorption capacity than the sisal fibers, which is favorable for the formation of a denser transition zone than expected for the sisal–cement interface.

The presence of the polymer film, in turn, reduces the elastic modulus of sisal fiber, as can be observed in *Table II*, and this can actually contribute to a reduction in the rigidity of the load–slip curve. Moreover, it appears from *Figure 3* that the surface of the treated fiber is smoother, which contributes to a reduction in adherence since a rougher surface enhances the mechanical interlocking adhesion between the fibers and the matrix materials [51].

During the pullout test, most of the axial force is applied to the sisal fiber, which transfers the internal efforts to the cement matrix through the CA film by means of shear stresses. The adhesion between the sisal fiber and the CA film plays a vital role in stress transfer and thus becomes crucial in determining the mechanical properties of the composites. However, it has been observed that for plant-based fiber composites, the interaction between the hydrophilic fibers and the polymer matrices, which are commonly hydrophobic, is usually limited; this leads to poor interfacial bonding, which, in turn, limits the mechanical performance [52]. Thus, during load application in the pullout test of the treated fiber, cracking occurs at the fiber–polymer interface, which induces a displacement of the fiber within the polymer, as shown in *Figure 12*, and a decrease in stiffness.

It can be verified that during the pullout process of the treated sisal fiber (embedded length of 40 mm), the polymer film breaks before the fiber, which is in agreement with the tensile strength and ultimate strain values listed *Table I* and *Table II*. After that, the load–displacement behavior is governed by two processes (*Figure 11*): pullout of the sisal fiber within the polymer film and gradual sliding of the treated fiber within the cement matrix.

In Regions 1–3, the treated fiber with an embedded length of 20 mm shows behavior similar to the untreated sisal fiber, despite the load reduction and stiffness. In Region 4, on the other hand, after the first debonding of the fiber, a sharp drop in force occurs and some peaks can be observed after a certain slip. A similar behavior has been observed in other studies [53, 54]; this behavior is not directly related to the fiber treatment. The load peaks can be attributed to the increase in the cross-sectional area of the natural fiber along the length, which leads to the development of larger stresses owing to the contribution of mechanical anchoring.

Analysis of the bond strength τ, calculated using Eq. (2) and listed in *Table II*, verifies that fiber treatment causes 40% and 47% reductions in τ for embedded lengths of 20 mm and 40 mm, respectively. However, extensive research has been conducted for achieving improved interfacial bonding between natural fiber and polymers. In order to improve the pullout bond of the polymer-treated sisal fiber, this treatment was performed after hornification of the fiber [46]. The results indicate a greater adhesion bond, which led to an increase of 75% in the adhesion strength in comparison to the fiber treated with only polymer.

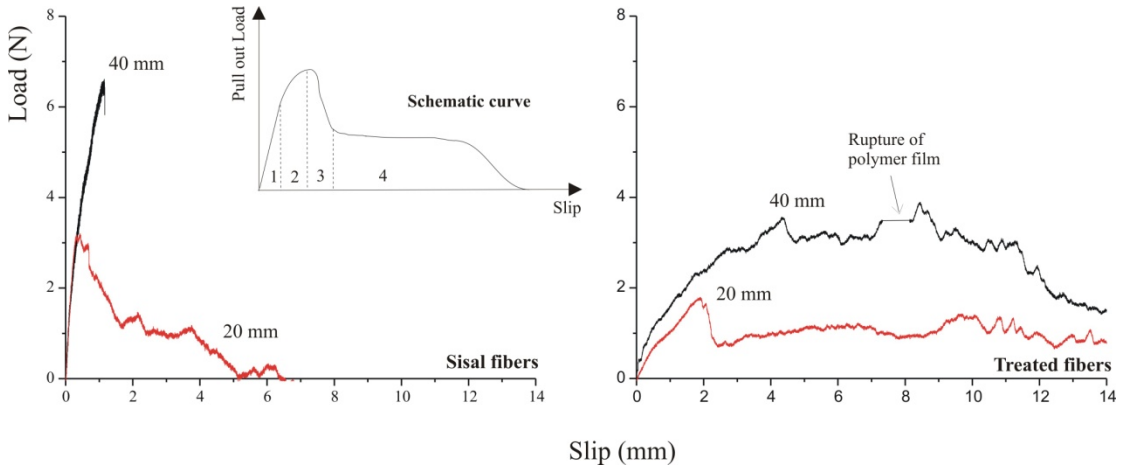

FIGURE 11. Tension-pull out curves of natural sisal fibers and treated (CA treatment) in cement matrix.

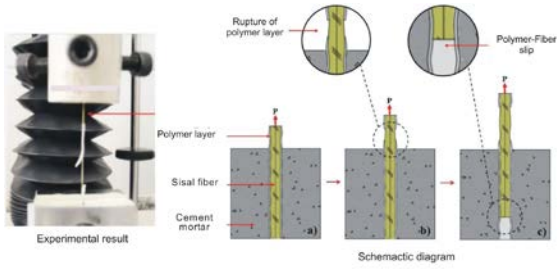

FIGURE 12. Schematic pull out behavior of treated fiber.

TABLE II. Pull out test results.

Treatment	Lf (mm)	P (N)	τ (MPa)
Untreated	20	3.24 (0.54)	0.15 (0.03)
	40	7.32 (3.02)	0.19 (0.04)
CA Treatment	20	2.00 (0.66)	0.09 (0.01)
	40	5.20 (1.05)	0.10 (0.02)

Flexural Test

Figure 13 shows the typical bending behavior of the composites reinforced with treated (CA treatment) and untreated sisal fibers with a 4% volume fraction.

Despite the use of a short fiber, the natural-fiber-reinforced composite exhibits multiple cracking behavior and quasi-plastic behavior under flexion, similar to that observed in a previous study [10]. This phenomenon can be explained by the adequate fiber–matrix interface that permits the transfer of stress between the cracked matrix and the sisal fiber reinforcement and by the consideration of a self-compacting matrix that permits the fabrication of composites that are more homogenous.

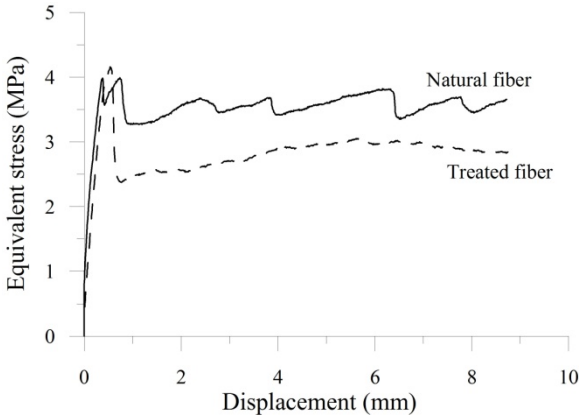

FIGURE 13. Effect of fiber treatment on the flexural behavior of sisal fiber cement composite.

In the composite reinforced with treated fiber, however, the flexural behavior is characterized by a larger drop in the load after the first crack. During the subsequent deformation, the treated-fiber-reinforced composite shows a single opening crack and rupture by pullout fiber of matrix. This fact confirms the reduction in the fiber–matrix bond stress as presented in *Table II* and results in a reduction in the toughness of the composites, as provided in *Table III*. The composite reinforced with treated fiber has approximately 4% higher flexural strength and up to 25% lower toughness than that reinforced with natural fiber. Despite this reduction in toughness, the dimensional changes of the fiber that may be induced by moisture variation are expected to reduce owing to the moisture resistance offered by the polymer film [46]; this may lead to better mechanical behavior of the treated-fiber-reinforced composite under weather conditions in comparison to the behavior of composites reinforced with untreated fiber.

TABLE III. Flexural test results.

Treatment	Flexural strentgh (MPa)	Toughness (N/mm)	
		$FT_{2\ mm}$	$FT_{5\ mm}$
Untreated	4.00 (6.12)	3.07 (0.30)	3.29 (0.15)
CA treatment	4.16 (3.72)	2.44 (0.17)	2.45 (0.22)

CONCLUSION

In this work, sisal fiber was subjected to separate treatments with three types of biopolymers—derived from cellulose acetate, cassava starch, and hydrophobic starch—as coupling agents to reduce the hydrophilicity of the fiber. All treatments resulted in a modification of the FTIR spectra of the fibers, indicating an alteration of the fiber surface by the treatment.

Results of a water absorption test showed that because of the hydrophilic nature of the cassava starch and hydrophobic starch films, the water absorption capacities of the sisal fibers treated with these biopolymers increased in comparison to that of untreated natural fiber, whereas fibers treated with the cellulose acetate film showed a significantly reduced water absorption capacity. Results of tensile tests of the fibers also indicated that the use of cellulose acetate led to lower losses of strength and stiffness of the sisal fiber in comparison to the use of the other two biopolymers. This is because according to the tensile test results of the biopolymer films, the cellulose acetate film showed higher strength and elastic modulus than did the cassava starch and hydrophobic starch films.

Despite the reduction in the hydrophilicity of the sisal fiber, its treatment with the cellulose acetate biopolymer modified the fiber pullout behavior in a cement matrix, with a reduction in the stiffness of the fiber–matrix interface and a reduction of up to 47% in the bond strength. A pullout test of a fiber with a longer embedded length revealed a rupture of the biopolymer film covering the fiber and the occurrence of subsequent fiber-film slipping, indicating a weak chemical bond between them.

As a result of the reduction in bond strength, the flexural behavior of the composite reinforced with treated fiber was characterized by a reduced toughness in comparison to that of a composite reinforced with natural fiber.

Therefore, it can be concluded that in order for the produced cellulose acetate biopolymer to be used as a coupling agent in the treatment of natural fiber, the biopolymer must be modified to ensure, besides a reduction in the hydrophilicity of the fiber, stronger film–matrix and film–fiber bonding.

ACKNOWLEDGMENT

The authors thank the National Council for Scientific and Technological Development (CNPq) for their financial support, FAPESB for the Masters scholarship of the second author, LAPRON/UEFS for their support in the performance of FTIR spectroscopy measurements, LABEST/COPPE for their support in the performance of SEM observations, and Solvay Company and Bahia Amido Company for donating the materials used.

REFERENCES

[1] Silva FA, Toledo Filho RD, Melo Filho JA, Fairbairn EDM. Physical and mechanical properties of durable sisal fiber–cement composites. Construction and Building Materials. 2010; 24:777-85.

[2] Bakare IO, Okieimen FE, Pavithran C, Abdul Khalil HPS, Brahmakumar M. Mechanical and thermal properties of sisal fiber-reinforced rubber seed oil-based polyurethane composites. Materials & Design. 2010; 31: 4274-80.

[3] Rao KM, Prasad AVR. Fabrication and testing of natural fibre composites: vakka, sisal, bamboo and banana. Materials and Design. 2010; 31:508–13.

[4] Ali M, Li X, Chouw N. Experimental investigations on bond strength between coconut fibre and concrete. Materials & Design. 2013; 44:596-605.

[5] Kannappan S, Dhurai B. Investigating and optimizing the process variables related to the tensile properties of short jute fiber reinforced with polypropylene composite board. Journal of Engineered Fibers and Fabrics. 2012; 7:28-34.

[6] Silva FA, Chawla N, Toledo Filho RD. Mechanical Behavior of Natural Sisal Fibers. Journal of Biobased Materials and Bioenergy. 2010; 4:106-13.

[7] Scopel F, Gregolin JAR, Faria LIL. Tendências tecnológicas do uso do sisal em compósitos a partir da prospecção em documentos de patentes. Polímeros. 2013; 23: 514-20.

[8] Tonoli GHD, Santos SF, Santos WN, Savastano Junior, H. Thermal performance of sisal fiber-cement roofing tiles for rural constructions, Scientia Agricola. 2011;68:1-7.

[9] Melo Filho, JA. Desenvolvimento e Caracterização de Laminados Cimentíceos Reforçados com Fibras Longas de Sisal. Thesis (Civil Engineering), COPPE/UFRJ, Rio de Janeiro, Brasil, 2012.

[10] Ferreira SR, Lima PRL, Silva FA, Toledo Filho RD. Effect of sisal fiber hornification on the fiber-matrix bonding characteristics and bending behavior of cement based composites. Key Engineering materials. 600 (2014) 421-432.

[11] Olivito RS, Cevallos OA, Carrozzini A. Development of durable cementitious composites using sisal and flax fabrics for reinforcement of masonry structures. Materials & Design. 2014; 57:258-68.

[12] Rong MZ, Zhang MQ, Liu Y, Yang GC, Zeng HM. The effect of fiber treatment on the mechanical properties of unidirectional sisal-reinforced epoxy composites. Composites Science and Technology. 2001; 61:1437-47.

[13] Bledzki AK, Reihmane S, Gassan J. Properties and modification methods for vegetable fibers for natural fiber composites. Journal of Applied Polymer Science. 1996; 59:1329-36.

[14] Toledo Filho RD, Ghavami K, England GL, Scrivener K. Development of vegetable fibre–mortar composites of improved durability. Cement & Concrete Composites. 2003; 25:185–96.

[15] Mai YW, Hakeem MI, Cotterell B. Effects of water and bleaching on the mechanical properties of cellulose fibre cements, J. Mater. Sci. 1983; 18:2156–62.

[16] Coutts RSP. Autoclaved beaten wooden fibre-reinforced cement composites. Composites. 1984; 15:139–43.

[17] Coutts RSP. Flax fibres as a reinforcement in cement mortars. Int. J. Cem. Comp. Ltwt. Concr. 1983;5:257–62.

[18] R.D. Toledo Filho. Natural fibre reinforced mortar composites: experimental characterization, PhD thesis, DEC-PUC-Rio, Brazil, 1997. p. 472.

[19] Belgacem MN, Gandini A. Surface Modification of Cellulose Fibres, In Monomers, Polymers and Composites from Renewable Resources. Elsevier, Amsterdan, 2008.

[20] Ferreira SR, Lima PRL, Silva FA, Toledo Filho RD. Effect of sisal fiber hornification on the adhesion with portland cement matrices. Materia. 2012; 17:1024-34.

[21] Motta LAC, John VM, Agopyan V. Thermo-mechanical treatment to improve properties of sisal fibres for composites. Materials Science Forum. 2010; 636:253-59.

[22] George J, Sreekala MS. A review on interface modification and characterization of natural fiber reinforced plastic composites. Polymer Engineering & Science. 2001; 41:1471-85.

[23] Cristaldi G, Latteri A, Recca G, Cicala G. Composites Based on Natural Fibre Fabrics, Woven Fabric Engineering, Polona Dobnik Dubrovski (Ed.), InTech, DOI: 10.5772/10465. Available from: http://www.intechopen.com/books/woven-fabric-engineering/composites-based-on-natural-fibre-fabrics, 2015.

[24] Canovas MF, Selva NH, Kawiche GM. New economical solutions for improvement or durability of Portland mortars reinforced with sisal fibres. Materials and Structures. 1992; 25: 417-22.

[25] Toledo Filho RD, Ghavami K, England GL, Scrivener K. Durability of alkali-sensitive sisal and coconut fibres in cement mortar composites. Cement and Concrete composites. 2000; 22:127-43.

[26] Zhou F, Cheng G, Jiang B. Effect of silane treatment on microstructure of sisal fibers. Applied Surface Science. 2014; 292:806-12.

[27] Faruka O, Bledzkia AK, Fink HP, Sain M. Biocomposites reinforced with natural fibers: 2000–2010. Progress in Polymer Science. 2012; 37:1552– 96.

[28] Singh B, Gupta M, Verma A. Influence of fiber surface treatment on the properties of sisal polyester composites. Polymer Composites. 1996; 17:910-8.

[29] John MJ, Thomas S. Biofibres and biocomposites. Carbohydrate Polymers. 2008; 71: 343–64.

[30] Flieger M, Kantorová M, Prell A, Řezanka T, Votruba J. Biodegradable plastics from renewable sources. Folia Microbiol. 2003; 48:27–44.

[31] Satyanarayana KG, Arizaga GGC, Wypych F. Biodegradable composites based on lignocellulosic fibers—An overview. Progress in Polymer Science. 2009; 34:982–1021.

[32] Mohanty AK, Misra M, Drzal LT. Sustainable Bio-Composites from Renewable resources: opportunities and challenges in the green materials world. Journal of Polymers and the Environment. 2002; 10:19-26.

[33] Zhang MQ, Rong MZ, Lu X. Fully biodegradable natural fiber composites from renewable resources: All-plant fiber composites, Composites Science and Technology. 2005; 65: 2514–25.

[34] Mohanty AK, Wibowo A, Misra M, Drzal LT. Effect of process engineering on the performance of natural fiber reinforced cellulose acetate biocomposites. Composites: Part A. 2004; 35:363–70.

[35] Camano S, Behary N, Vroman P, Campagne C. Comparison of Bio and Eco-technologies with Chemical Methods for Pre-treatment of Flax Fibers: Impact on Fiber Properties. Journal of Engineered Fibers and Fabrics. 2014; 9:56-67.

[36] Disponible in: http://www.science.marshall.edu/murraye/alpha_amylase.htm. Accessible in 20 may 2016.

[37] Lima PRL, Toledo Filho RD. Uso de metacaulinita para incremento da durabilidade de compósitos à base de cimento reforçados com fibras de sisal. Ambiente Construído. 2008; 8:7-19.

[38] ABNT NBR 13276:2005. Mortars applied on walls and ceilings - Preparation of mortar for unit masonry and rendering with standard consistence index. Rio de Janeiro, 3p.

[39] Santos RJ, Lima PRL. Effect of treatment of sisal fiber on morphology, mechanical properties and fiber-cement bond strength. Key Engineering Materials. 2014; 634:410-410.

[40] Lima PRL. Análise teórica e experimental de compósitos reforçados com fibras de sisal. Thesis (Civil Engineering) COPPEDEC/UFRJ, 2004. 263p.

[41] Herrera-Franco PJ, Valadez-Gonzalez A. A study of the mechanical properties of short natural-fiber reinforced composites. Composites: Part B. 2005; 36: 597–608.

[42] Kim JT, Netravali AN. Mercerization of sisal fibers: Effect of tension on mechanical properties of sisal fiber and fiber-reinforced composites. Composites part: A. 2010; 41: 1245-52.

[43] Mohan TP, Kanny K. Chemical treatment of sisal fiber using alkali and clay method. Composites: Part A. 2012; 43:1989–98.

[44] Zhang C, Zhong S, Yang Z. Cellulose acetate-based molecularly imprinted polymeric membrane for separation of vanillin and o-vanillin. Brazilian Journal of Chemical Engineering.2008; 25:365-73.

[45] Delval F, Crini G, Bertini S, Morin-crini N, Badot PM, Vebrel J, Torri G. Characterization of crosslinked starch materials with spectroscopic techniques. Journal of Applied Polymer Science. 2004; 93:2650-63.
[46] Ferreira SR, Silva FA, Lima PRL, Toledo Filho RD. Effect of fiber treatments on the sisal fiber properties and fiber–matrix bond in cement based systems. Construction and Building Materials.2015; 101:730-40.
[47] Teodoroa AP, Mali S, Romeroa N, Carvalho GM. Cassava starch films containing acetylated starch nanoparticles as reinforcement: Physical and mechanical characterization. Carbohydrate Polymers. 2015; 126: 9–16.
[48] Belaadi A, Bezazi A, Bourchak M, Scarpa F. Tensile static and fatigue behaviour of sisal fibres. Materials & Design. 2013; 46:76-83.
[49] Lima PRL, Santos RJ, Ferreira SR, Toledo Filho RD. Characterization and treatment of sisal fiber residues for cement-based composite application. Engenharia Agrícola. 2014; 34:812-25.
[50] Abtahi SM, Esfandiarpour A, Kunt M, Hejazi SM, Ebrahimi MG. Hybrid reinforcement of asphalt-concrete mixtures using glass and polypropylene fibers. Journal of Engineered Fibers and Fabrics. 2013; 8:25-35.
[51] Zhou F, Cheng G, Jiang B. Effect of silane treatment on microstructure of sisal fibers. Applied Surface Science. 2014; 292:806-12.
[52] Pickering KL, Efendy MA, Le TM. A review of recent developments in natural fibre composites and their mechanical performance. Composites Part A: Applied Science and Manufacturing. 2016; 83:98-112.
[53] Yang L, Thomason JL. Development and application of micromechanical techniques for characterising interfacial shear strength in fibre-thermoplastic composites. Polymer Testing. 2012; 31:895-903.
[54] Lecompte T, Perrot A, Subrianto A, Le Duigou A, Ausias G. A novel pull-out device used to study the influence of pressure during processing of cement-based material reinforced with coir. Construction and Building Materials 2015; 78:224-33.

AUTHORS' ADDRESSES
Paulo R. L. Lima, PhD
Heni Mirna Santos
Geany Peruch Camilloto PhD
Renato Souza Cruz PhD
State University of Feira de Santana Technology
Av. Transnordestina, s / n - Novo Horizonte
Feira de Santana, Bahia 44036 – 900
BRAZIL